Automated machine learning to evaluate the information content of tropospheric trace gas columns for fine particle estimates over India: a modeling testbed

Zhonghua Zheng[1], Arlene M. Fiore[1,2,3,4], Daniel M. Westervelt[1,3,5], George P. Milly[1], Jeff Goldsmith[3,6], Alexandra Karambelas[1], Gabriele Curci[7,8], Cynthia A. Randles[9], Antonio R. Paiva[9], Chi Wang[10], Qingyun Wu[11], Sagnik Dey[12,13]

[1]Lamont-Doherty Earth Observatory, Columbia University, USA

[2]Department of Earth and Environmental Sciences, Columbia University, USA

[3]Data Science Institute, Columbia University, USA

[4]Department of Earth, Atmospheric and Planetary Sciences, Massachusetts Institute of Technology, USA

[5]NASA Goddard Institute for Space Studies, USA

[6]Department of Biostatistics, Columbia University, USA

[7]Department of Physical and Chemical Sciences, University of L'Aquila, Italy

[8]Center of Excellence in Telesensing of Environment and Model Prediction of Severe events (CETEMPS), University of L'Aquila, Italy

[9]ExxonMobil Research and Engineering Company, USA

[10]Microsoft Corporation, USA

[11]College of Information Sciences and Technology, Pennsylvania State University, USA

[12]Centre for Atmospheric Sciences, Indian Institute of Technology Delhi, Hauz Khas, New Delhi, India

[13]Centre of Excellence for Research on Clean Air, Indian Institute of Technology Delhi, Hauz Khas, New Delhi, India

Corresponding author: Zhonghua Zheng (zhonghua.zheng@outlook.com)

Key Points:

- We developed an Automated Machine Learning workflow to evaluate the utility of incorporating multiple trace gas columns in $PM_{2.5}$ estimates
- Tropospheric trace gas columns contain signatures of $PM_{2.5}$ precursors and improve $PM_{2.5}$ estimates
- We infer the regional dominance of primary versus secondary sources of $PM_{2.5}$ using AutoML and Spearman's ranking correlation

Abstract

India is largely devoid of high-quality and reliable on-the-ground measurements of fine particulate matter ($PM_{2.5}$). Ground-level $PM_{2.5}$ concentrations are estimated from publicly available satellite Aerosol Optical Depth (AOD) products combined with other information. Prior research has largely overlooked the possibility of gaining additional accuracy and insights into the sources of PM using satellite retrievals of tropospheric trace gas columns. We first evaluate the information content of tropospheric trace gas columns for $PM_{2.5}$ estimates over India within a modeling testbed using an Automated Machine Learning (AutoML) approach, which selects from a menu of different machine learning tools based on the dataset. We then quantify the relative information content of tropospheric trace gas columns, AOD, meteorological fields, and emissions for estimating $PM_{2.5}$ over four Indian sub-regions on daily and monthly time scales. Our findings suggest that, regardless of the specific model assumptions, incorporating trace gas modeled columns improves $PM_{2.5}$ estimates. We use the ranking scores produced from the AutoML algorithm and Spearman's rank correlation to infer the relative dominance of primary versus secondary sources of $PM_{2.5}$ as a first step towards estimating particle composition. Our comparison of AutoML-derived models to selected baseline machine learning models demonstrates that AutoML is at least as good as model selection and hyperparameter tuning prior to training. The idealized pseudo-observations used in this work lay the groundwork for applying satellite retrievals of tropospheric trace gases to estimate fine particle concentrations in India and serve to illustrate the promise of AutoML applications in atmospheric and environmental research.

Plain Language Summary

Ground-level fine particle ($PM_{2.5}$) concentrations are frequently estimated with freely available satellite Aerosol Optical Depth (AOD) products. We focus on India where sparse ground-based monitoring leaves gaps in our understanding of particle concentrations and the relative importance of different sources. We use an atmospheric chemistry model to test whether satellite retrievals of tropospheric trace gas columns can provide information on the origins of $PM_{2.5}$ and improve satellite-derived. We created an Automated Machine Learning (AutoML) workflow to evaluate the utility of incorporating multiple trace gas columns in $PM_{2.5}$ estimates, which represents nonlinear relationships between predictands and predictors while freeing users from selecting and tuning a specific machine learning model. On daily and monthly time scales, we quantify the relative information content of trace gas columns, AOD, meteorological fields, and emissions. We find that incorporating trace gas columns improves $PM_{2.5}$ estimates and may also enable inference of broad characteristics of particle composition.

1 Introduction

High levels of ambient fine particles (known as $PM_{2.5}$, particles 2.5 μm in diameter or smaller) pose a major environmental issue in India. As estimated by Chowdhury et al., (2019), nearly the entire population (99.9%) in India is exposed to annual $PM_{2.5}$ exceeding the previous World Health Organization (WHO) guideline of 10 μg/m^3. The latest WHO Global Air Quality Guidelines (AQG) announced on September 22, 2021, has lowered the annual AQG level of $PM_{2.5}$ to 5 μg/m^3 (World Health Organization, 2021). To tackle the issue of air pollution, the Government of India launched the National Clean Air Program (NCAP) in January 2019, aimed at reducing particulate pollution by 20-30% relative to 2017 levels by 2024. Monitoring air quality and understanding pollutant sources are critical to implementing effective air quality management plans, but India mostly lacks long-term, publicly accessible, reliable (i.e., quality controlled) measurements of particle composition that enable source attribution (Bali et al., 2021; Brauer et al., 2019). Although the Central Pollution Control Board (CPCB) has maintained a routine monitoring network for total $PM_{2.5}$ mass (composition unknown) and certain gas-phase species since 2008, the density of India's monitoring network (~0.14 monitors/million persons) is lower than other developing countries such as China (1.2 monitors/million persons) and developed countries such as USA (3.4 monitors/million persons), and leaves the majority of rural India entirely unmonitored (Bali et al., 2021; Brauer et al., 2019; Karambelas et al., 2018; Ravishankara et al., 2020).

Publicly available satellite products offer the opportunity to overcome limitations in spatiotemporal coverage and estimate $PM_{2.5}$ across India by combining satellite data with other information. Satellite aerosol optical depth (AOD) is often used to estimate $PM_{2.5}$ (van Donkelaar et al., 2006; Hoff & Christopher, 2009). Columnar AOD is combined with geophysical or statistical models that ingest additional meteorological data, emission inventories, chemical transport model simulations, and/or land use to estimate $PM_{2.5}$ and achieve better performance (Brauer et al., 2016; Xu et al., 2015). Typically, these approaches require high-quality ground-based measurements for model training and validation, which is not possible in India due to the country's low monitor density relative to other world regions (e.g., U.S. and China).

Importantly, the possibility of gleaning additional insights into sources of PM from satellite retrievals of tropospheric trace gases has generally been overlooked. Trace gases including sulfur dioxide, nitrogen dioxide, and ammonia are precursors to fine particles that form via chemical reactions and thus should indicate the potential to form secondary PM. Other trace gases such as carbon monoxide (a product of incomplete combustion) and formaldehyde (produced during the oxidation of numerous organic gases) may correlate with emissions of aerosols or their precursor gases and may thus indicate primary (directly emitted) PM, as well as transported pollution of particles emitted or produced upwind. Thus we evaluate here the potential for incorporating trace gas tropospheric columns into statistical approaches to increase the accuracy of ground-level $PM_{2.5}$ estimates in India. In this first study, we use a model as a testbed to assess the potential information content in tropospheric trace gas columns retrieved from satellite instruments.

Artificial intelligence (AI) and data science methods, and machine learning (ML) methods in particular, have been developed and used in atmospheric and environmental studies over the last few years. This trend is likely to persist into the foreseeable future enabled by the rapid advances and tremendous needs in many areas, such as weather forecasting and predictions (Agrawal et al., 2019; Lagerquist et al., 2019; McGovern et al., 2017), Earth system modeling (Gentine et al., 2021; Irrgang et al., 2021; Reichstein et al., 2019), and climate analysis (Labe & Barnes, 2021; Toms et al., 2020). As an alternative to simple geophysical or statistical approaches, ML approaches such as Random Forest and Gradient Boosting have been applied to meld satellite estimates of aerosol optical depth (AOD) with weather and land use data to produce highly spatially and temporally resolved datasets to develop surface $PM_{2.5}$ concentration (Di et al., 2019; Geng et al., 2020; Rybarczyk & Zalakeviciute, 2018; Xiao et al., 2018). According to the "*No Free Lunch* (NFL)" theorem (Wolpert, 1996), no one ML algorithm can be universally good for all data and problems. Instead, the nature of the problem, the data, and the purpose synergistically determine the appropriate learning algorithm for a problem. For example, a deep-learning-based model architecture trained to predict severe weather might not successfully predict an extreme air pollution episode. In some cases, given the sensitivity of the data-driven models, incorporating new predictors could shift the "ideal" learning algorithm from one to another (e.g., from linear to nonlinear). Even if the "best" learning algorithm is predefined (e.g., a neural network or a gradient boosting model), searching and tuning the hyperparameters (e.g., number of hidden layers in a neural network, or the learning rate of a gradient boosting model) usually depends on human knowledge and decisions. Furthermore, ML approaches generally require significant computational resources to implement.

Concerns with machine learning computational efficiency have given rise to fast and economical software frameworks, known as Automated Machine Learning (AutoML) (Wang et al., 2021), in which "the user simply provides data, and the AutoML system automatically determines the approach that performs best for this particular application" (Hutter et al., 2019). AutoML frees domain scientists from selecting learners and hyperparameters and can potentially prevent suboptimal choices due to idiosyncrasies or ad-hocness. For example, Adams et al. (2020) have successfully employed AutoML (an R package "H2O") for an optimal solution to correct low-cost air quality sensors.

In this study, we leverage the power of AutoML to evaluate the added benefit of satellite retrieval of tropospheric trace gases in $PM_{2.5}$ estimates over India. We use a chemical transport model as a synthetic testbed for developing methods under spatially and temporally continuous ("perfect") datasets and use the AutoML as a tool to fit the regression of surface $PM_{2.5}$ given the meteorological fields, emission inventory, and satellite-like pseudo-datasets sampled from the model. Note the overarching goal of this study is not to provide regression models or $PM_{2.5}$ products. Instead, we aim to assess the improved accuracy that may be possible by incorporating satellite retrievals of tropospheric trace gases, thereby providing guidance for developing future $PM_{2.5}$ products by blending together multiple datasets, especially over regions lacking widespread networks of particle mass and composition measurements.

2 Methods

2.1 GEOS-CHEM simulations and Data Processing

We use simulations from the GEOS-Chem version 12.0.2 (The International GEOS-Chem User Community, 2018) chemical transport model as idealized pseudo-observations continuously available from ground-based and space-based platforms. The simulations were conducted for the year 2015 with a global 2° latitude x 2.5° longitude domain providing boundary conditions to a nested grid (0.25° latitude x 0.3125° longitude, ~25km x 30 km) and 47 non-uniform vertical layers over India (0-40° N and 60-100° E) as described in Karambelas et al. (2022). This nested grid configuration was loosely based on (Chaliyakunnel et al., 2019), which used the MERRA-2 reanalysis meteorology. Instead, we use GEOS-FP fields to achieve higher spatial resolution (Karambelas et al., 2022). We use the standard tropospheric and stratospheric chemistry (e.g., NO_X-O_X-HC-aerosol-Br with a simple secondary organic aerosol representation) and physics (Pai et al., 2020; Prashanth et al., 2021), and natural and biogenic emissions. Anthropogenic emissions are from the ECLIPSE anthropogenic emission inventory (Stohl et al.,

2015) processed through the Harvard-NASA Emissions Component (HEMCO) (Keller et al., 2014). More information on the simulations can be found at Karambelas et al. (2022).

We construct surface $PM_{2.5}$ concentrations from the individual simulated chemical components (ammonium, nitrate, sulfate, black carbon, organic carbon, secondary organic aerosols, dust, and sea salt), and assume a relative humidity of 50%. We develop "pseudo-datasets" by sampling modeled fields at satellite overpass time. These datasets are "perfect" in the sense that no instrument noise or missed retrievals are introduced (e.g. due to clouds, etc.). Specifically, we use the Flexible Aerosol Optical Depth (FlexAOD) post-processing tool (Curci et al., 2015) to estimate aerosol optical depth (AOD) at 550 nm and dust AOD. These fields are sampled at 5:00 AM UTC to coincide with Terra's local 10:30 AM overpass. The tropospheric vertical columns (troposphere is defined as from the surface layer to model level 38) of trace gases (CO, SO_2, NO_2, CH_2O, and NH_3) are sampled at 8:00 AM UTC to match satellite instruments with a local 1:30 PM overpass. Meteorological fields were averaged on a daily and a monthly basis for further analysis. The emission fields without daily variation were only used for monthly analyses. Table 1 lists the fields (features) used in our analyses. Note that the months April and August were used as the hold-out samples (testing data) for validation purposes, and the remaining ten months (including PM episodes that happened in December) were used for the regionalization (see Section 2.2) and training in the Automated Machine Learning (AutoML) workflow. We restrict our analysis to land grid cells (defined as land covering a fraction greater than 0.5 of any individual cell).

Table 1. Features (fields) definitions.

Type	Feature (fields)	Description	Temporal resolution
Meteorological	T2M	2-meter air temperature	Daily and Monthly
	RH	2-meter relative humidity	
	PBLH	Planetary boundary layer height	
	U10M	10-meter eastward wind	
	V10M	10-meter northward wind	
	PRECTOT	Total precipitation	
Satellite (aerosol)	AOT_C	Aerosol optical thickness (or AOD) at 550 nm	
	AOT_DUST_C	Aerosol optical thickness (or AOD) of dust at 550 nm	
Satellite (trace gases)	CO_trop	tropospheric vertical column of CO	
	SO2_trop	tropospheric vertical column of SO2	
	NO2_trop	tropospheric vertical column of NO2	
	CH2O_trop	tropospheric vertical column of CH2O	
	NH3_trop	tropospheric vertical column of NH3	
Emission	EmisDST_Natural	Dust emissions from natural sources (EmisDST1_Natural+ EmisDST2_Natural+ EmisDST3_Natural+ EmisDST4_Natural), number indicates GEOS-Chem size bin	
	EmisNO_Fert	NO emissions from fertilizer	
	EmisNO_Lightning	NO_emissions_from_lightning	
	EmisNO_Ship	NO emissions from ships	
	EmisNO_Soil	NO emissions from soil	
	EmisBC_Anthro	Black carbon aerosol emissions from anthropogenic sources	Monthly

		(EmisBCPI_Anthro+ EmisBCPO_Anthro), "PI" refers to "hydrophilic" and "PO" refers to "hydrophobic"	
	EmisBC_BioBurn	Black carbon aerosol emissions from biomass burning (EmisBCPI_BioBurn+ EmisBCPO_BioBurn)	
	EmisOC_Anthro	Organic carbon aerosol emissions from anthropogenic sources (EmisOCPI_Anthro+ EmisOCPO_Anthro)	
	EmisOC_BioBurn	Black carbon aerosol emissions from biomass burning (EmisOCPI_BioBurn+ EmisOCPO_BioBurn)	
	EmisCH2O_Anthro	Formaldehyde (CH2O) emissions from anthropogenic sources	
	EmisCH2O_BioBurn	CH2O emissions from biomass burning	
	EmisCO_Anthro	CO emissions from anthropogenic sources	
	EmisCO_BioBurn	CO emissions from biomass burning	
	EmisCO_Ship	CO emissions from ships	
	EmisNH3_Anthro	NH3 emissions from anthropogenic sources	
	EmisNH3_BioBurn	NH3 emissions from biomass burning	
	EmisNH3_Natural	NH3 emissions from natural sources	
	EmisNO_Aircraft	NO emissions from aircraft	
	EmisNO_Anthro	NO emissions from anthropogenic sources	
	EmisNO_BioBurn	NO emissions from biomass burning	
	EmisSO2_Aircraft	SO2 emissions from aircraft	
	EmisSO2_Anthro	SO2 emissions from anthropogenic sources	
	EmisSO2_BioBurn	SO2 emissions from biomass burning	
	EmisSO4_Anthro	SO4 emissions from anthropogenic sources	

2.2 Delineating geographical regions

We perform regional analysis to facilitate comprehension of spatial patterns. Rather than define regions for our analysis based on prior studies, for example, based on climate regions (Hu et al., 2017) or $PM_{2.5}$ concentrations (Greenstone et al., 2015), we propose a simple data-driven unsupervised learning approach for regionalization (Figure 1). Our approach groups grid cells into a few regions (clusters) based on their spatiotemporal similarity. The regionalization consists of two steps: (1) Empirical Orthogonal Functions (EOFs) and Varimax rotated EOFs (REOFs) analysis to reduce the dimensionality of the dataset and capture the spatiotemporal patterns, and (2) *k*-means clustering to identify common regional patterns of variability across the EOFs.

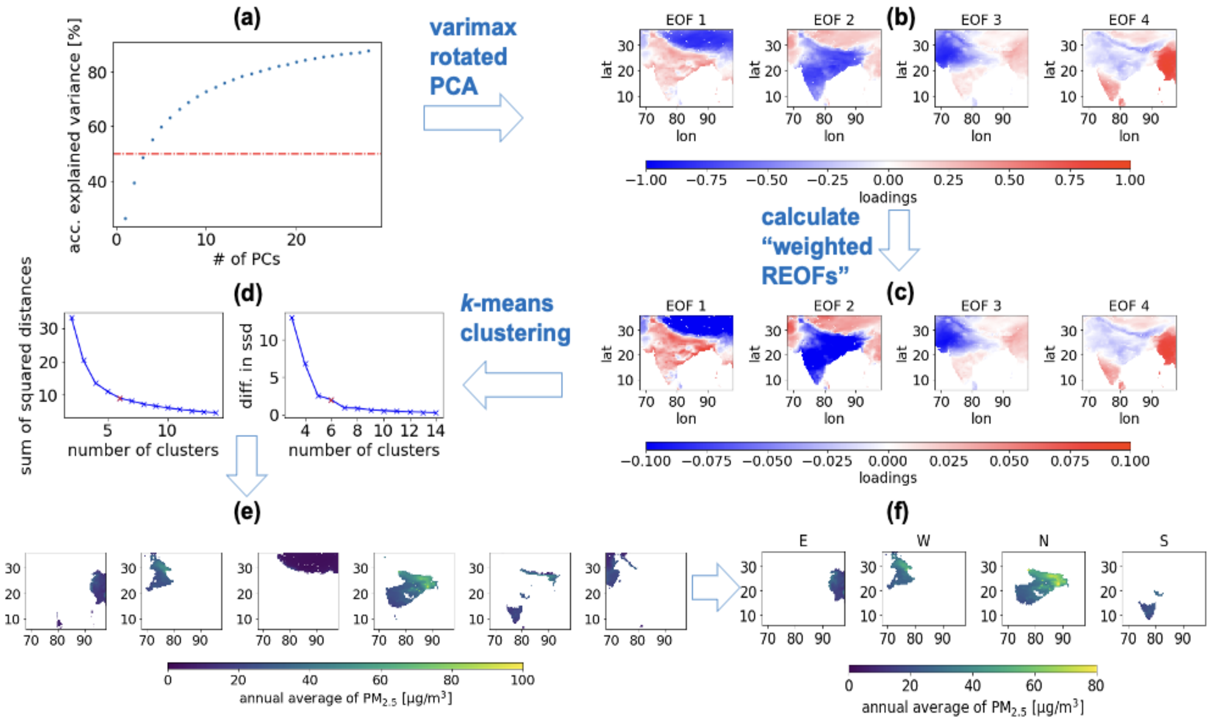

Figure 1. **The workflow of delineating geographical regions.** (a) PCA to derive the EOFs that capture over 50% of the variance (first four EOFs); (b) Varimax-rotated loadings for the selected EOFs; (c) Weighted averaged loadings for the selected EOFs; (d) “Elbow method” to determine the number of regions (clusters); (e) Regions based on k=6 from k-means clustering; (f) Four regions that intersect with India’s land pixels.

2.2.1 EOF and REOF analysis

Compared to supervised learning, where model performance is evaluated by a set of metrics (e.g., root-mean-square error) against validation datasets, unsupervised learning does not lend itself to quantitative evaluation. The principal component analysis (PCA) and its variant “varimax rotated PCA” have been widely applied in atmospheric and climate research, such as decomposing sea surface temperature (Lian & Chen, 2012) into REOFs to determine modes of variability. Motivated by a previous application of REOFs on the observed patterns of surface ozone (O_3) in the eastern United States (Fiore et al., 2003, 2021), we first applied PCA to derive the EOFs that capture over 50% of the variance (first four EOFs) in $PM_{2.5}$, then varimax-rotated the first four EOFs.

2.2.2 *k*-means clustering

The *k*-means clustering is an unsupervised learning approach and has been applied for ecoregion delineation (Kumar et al., 2011), environmental risk zoning (Shi & Zeng, 2014), and aerosol mixing state regionalization (Zheng et al., 2020). Qualitatively, we gauge successful implementations of clustering by the emergence of spatially contiguous regions without the direct guidance of spatial information (e.g., providing the algorithm with latitude and longitude). We multiply the EOF loadings by the corresponding explained variance to produce "weighted EOFs" as the input for the *k*-means clustering so that Euclidean distances among them correctly capture the relationships with respect to the original feature space. We use the "elbow method" to identify an optimal trade-off point and select six clusters (Hastie et al., 2009). Then we select four regions that intersect with India's land pixels as our study areas. Note that the four regions (Fig. 1e) contain not only India but also nearby countries, such as Bangladesh, Nepal, and Myanmar. Additionally, Region C (the union of four regions) and Region A (India and its neighbors, including all land grid cells from the simulations) are considered in this study to examine patterns at various spatial scales (see Section 2.4).

2.3 Automated Machine Learning (AutoML)

Rather than using a specific machine learning approach (e.g., Random Forest) to build regression models and quantify the importance of various features (fields), here we use a lightweight Python library "FLAML" (a Fast and Lightweight AutoML library) (Wang et al., 2021) as the tool for the AutoML task. This library chooses a search order optimized for both computational cost and model error, and selects the learner, hyperparameters, sample size, and resampling strategy iteratively. When tested on a large open-source AutoML benchmark, FLAML has superior performance compared to the top-ranked AutoML libraries, but with much smaller computational and time budgets (Wang et al., 2021). Given our modeling formulation, we configured the AutoML for a regression task with "auto" for the estimator list, optimizing the R^2 metric, and assigned a time budget of "5400 seconds" (1.5 hours) for each AutoML experiment. The "auto" scheme of ML estimator models consists in this library of tree-based approaches, namely, LightGBM (Light Gradient Boosting Machine, Ke et al., 2017), XGBoost (eXtreme Gradient Boosting, Chen & Guestrin, 2016), CatBoost (categorical boosting, Prokhorenkova et al., 2018), Random Forests (Breiman, 2001), and Extra-Trees (Extremely randomized trees, Geurts et al., 2006). We then compare the best estimator (the specific learning algorithm/model with the best result on the held-out validation data) from AutoML with two baseline models: the default configurations of XGBoost and Random Forests.

2.4 Experimental Design

We conduct a series of comparisons and answer three core questions by using the best estimators trained from AutoML (Table 2). First, the maximum benefit of tropospheric trace gas columns (using modeled proxies as described in Section 2.1) for surface $PM_{2.5}$ estimates can be determined by assessing the improvement in estimator performance when trace gas columns are used as features, in addition to meteorological variables, emissions, and AOD. We also test the model performance in the absence of AOD (removing total and dust AOD) when trace gases, meteorological variables, and emissions are available. Second, the same feature combination but different data (monthly versus daily) can be used to estimate the maximum information content possible from tropospheric trace gas columns and other input variables (using "perfect" model datasets) at different time scales. Monthly estimates, in comparison to daily estimates, attempt to capture spatial patterns and seasonal cycles but are unable to incorporate daily weather data. Third, the best estimators trained on data at different-sized regions ingested on different temporal averaging periods (monthly versus daily) provide insights on whether any benefit from including tropospheric trace gas columns is spatially equivalent.

Table 2. Experimental design and core questions.

	Feature	**Time Scale**	**Region**
Core Questions	Do tropospheric trace gases improve $PM_{2.5}$ estimates?	How does the ranking of features vary at different time scales?	How does the ranking of features vary in different regions?
Experiments	Data from the collection of all the grid cells falling into a certain region: - with trace gas columns - without trace gas columns but with AODs - with trace gas columns but without AODs	- daily - monthly	- E/S/W/N: individual region from Figure 2(f) - C: the union of four regions (E + S + W + N) - A: India and the neighboring countries (all land grid cells from the simulations, including Region C)

2.5 Feature Importance Attribution

In Data Science, "feature importance" refers to a score that represents how useful the feature is at predicting the target variable. However, the type of feature importance score differs for different learning algorithms and results in values with varying orders of magnitude. For example, the feature importance of Extra-Trees is based on "impurity" (the normalized total reduction of the mean squared error brought by that feature), LightBGM's feature importance is by default based on "split" (the numbers of times the feature is used in a tree node in the model), and XGBoost usually uses "gain" (the average Gini impurity/information gain across all splits the feature is used in).

Here we derive a metric, "ranking score," to unify the comparison of feature importance from different learning algorithms (e.g., Extra-Trees, LightGBM, and XGB). For each estimator, we rank the feature importance values from lowest to highest and assign a "ranking score" to each feature based on the rank order of the corresponding feature importance value. That is, the least important feature has a score of 1, the second to least important feature has a score of 2, and so on. As a result, ranking scores are bounded between 1 (least important) and the number of features (most important), which converts the feature importance of different estimators to the same scale for comparison. We also group features within the same type (Table 1) and compute the mean ranking score and the standard deviation within each type.

3 Results and Discussion

3.1 Including multiple trace gas modeled columns generally improves $PM_{2.5}$ estimates

We first evaluate whether $PM_{2.5}$ estimates improve in accuracy when we add trace gas tropospheric columns simulated by the GEOS-Chem model to the simulated meteorological variables, AOD, and emissions. We apply AutoML-derived nonlinear models and linear regression (LR). The coefficient of determination (R^2, based on an ordinary least-squares regression) between $PM_{2.5}$ simulated by GEOS-Chem versus that predicted with machine learning approaches is used as a metric for accuracy. These regressions provide average estimates, across the study area and time scales, of the association between trace gas columns and $PM_{2.5}$. As a comparison, we also apply the same approach to AODs.

While the "best estimator" from AutoML varies in space and time, we observe an increase in R^2 when simulated columnar trace gases are included in nonlinear and linear regression models (Fig. 2), implying that trace gases contain signatures useful for $PM_{2.5}$ estimation. However, including AODs as features in the presence of trace gas columns does not guarantee improved performance, and sometimes impairs the model performance (e.g., the difference between "GA" (both trace gas columns and AODs are available) and "G" (trace gas columns are available but AODs are not available) in monthly Region N). Given that the models with nonlinear relationships exhibit higher R^2 compared to the linear model, here we focus on the results from AutoML. The analysis of different ML model assumptions is discussed in Section 3.4. Some emission inventories in the model are only available at the monthly resolution, while others vary day-by-day. By comparing the results of monthly $PM_{2.5}$ estimates using only the emissions available at daily time scales ('Monthly (same features as Daily)') versus all emission inventories ('Monthly'), we find that using "all emission inventories" yields higher R^2 (e.g., 0.02 to 0.15 improvement in R^2 for "GA") at monthly time scales, implying that more accurate emission inventories (captured by the monthly emission features) will improve $PM_{2.5}$ estimates. In the following sections, we will keep the "Monthly" results that utilized emission data available at both monthly and daily time scales for analysis, since they yielded the best overall estimates of $PM_{2.5}$ in this study.

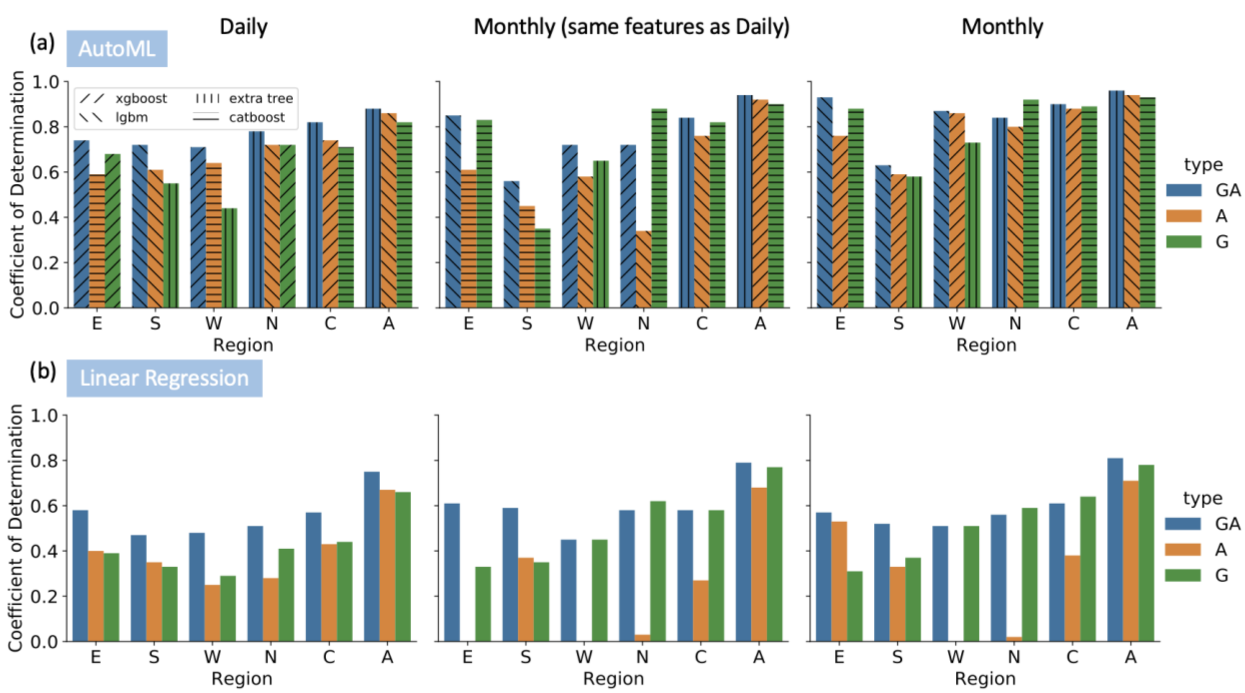

Figure 2. Improved predictive capability of $PM_{2.5}$ estimates when adding trace gas columns to other feature types in Table 1. Estimators are trained based on (a) AutoML and (b) linear regression. The left and middle panels differ in time scale (daily v.s. monthly), and the middle

and right panels differ in feature numbers (see Section 2.1 and Table 1). GA: both trace gas columns and AODs are available; A: AODs are available but trace gas columns are not available; G: trace gas columns are available but AODs are not available. Note the bars with the coefficient of determination lower than 0 are not shown, and results are based on testing data.

The improvements in R^2 vary spatially and temporally at the regional scale. In Region E, adding trace gas columns alongside AOD (GA) boosted daily R^2 from 0.59 to 0.74, and monthly from 0.76 to 0.93 compared to AOD alone (A). But in Region W, the increases in R^2 are moderate (+0.07 for daily and +0.01 for monthly). Given that other features already account for 86% of the variance in Region W on the monthly scale, adding trace gases only results in marginal increases in R^2 (note the improvement is not a linear addition, it reconstructs the interactions among all features, not only the interactions between other features and trace gases). Marginal increases in R^2 also occur for Region N, where the daily and monthly increases are 0.06 and 0.04, respectively. The increases in R^2 are not proportional to the baseline (without trace gases; A). For example, although the baseline monthly R^2 in Region S is relatively low, its increase is similar to other regions. The lower R^2 values for monthly $PM_{2.5}$ estimates in Region S may be due to insufficient samples, as this region's sample size is approximately one-fifth to half that of the other regions.

When training on data from the union of our four individual regions (Region C) or all the land grid cells as a whole (Region A), the inclusion of trace gases always contributes to a higher R^2. Especially, trace gases in Region C increased R^2 from 0.74 to 0.82 at the daily scale. At a larger geospatial scale (Region A), although the baseline R^2 values on the daily scale (0.86) and monthly scale (0.94) are well explained by meteorological fields, emission inventory, and AODs, the presence of trace gas columns can further explain variance (0.02 for both) in $PM_{2.5}$ and improve the estimates. However, a cost may be associated with the minor improvement, depending on the effort required to acquire additional data. As such, it is necessary to weigh the trade-offs.

3.2 The relative importance of trace gas columns to accurate $PM_{2.5}$ estimates varies spatially and temporally

We compare ranking scores among the types (Figure 3) and features (Figures 4 and 5), defined in Table 1, to study the relative importance of trace gas columns for improving $PM_{2.5}$ estimates over India, where a type or feature with a higher ranking score indicates its higher importance compared to other types or features in the regression. The ranking scores shown in Figures 3 - 5 suggest that the important features and feature interactions differ in space and time, which may be explained by regional and temporal differences in the dominant sources and the interactions with meteorological conditions.

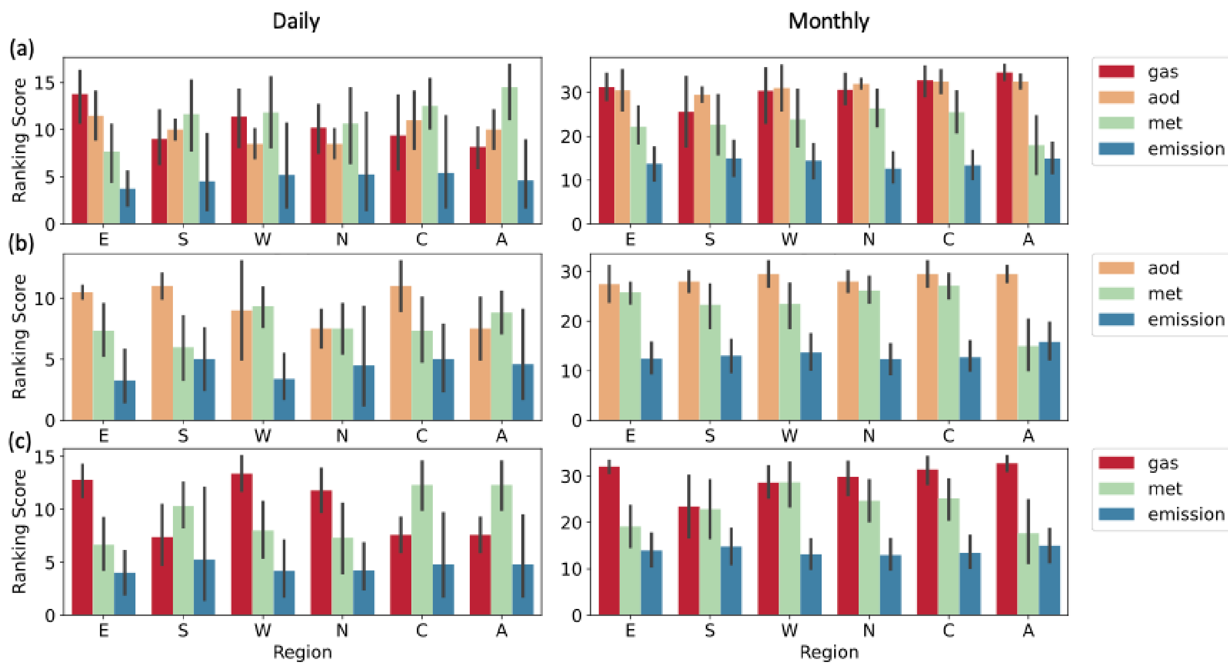

Figure 3. Ranking scores of AODs, meteorological fields, emission inventory, and trace gas column simulated by the GEOS-Chem model in estimating modeled $PM_{2.5}$. (a) both trace gas columns and AODs are available; (b) AODs are available but trace gas columns are not available; (c) trace gas columns are available but AODs are not available. Means and standard deviations of the ranking scores are derived from AutoML-trained "best estimators" within the same type.

On a daily scale, trace gas columns from GEOS-Chem (NO_2, SO_2, CH_2O, and NH_3) are the most important factors that boost the performance of $PM_{2.5}$ estimates in Region E (Figure 4). The order of other types remains similar (Figure 3) when trace gas columns or AODs are not included as features in this region. Region S, however, shows that the inclusion of the trace gas columns rearranges the order of feature importance among types (Figure 3). Without the use of trace gas columns to estimate daily $PM_{2.5}$ levels, the most significant feature type is AOD, followed by meteorological fields and emissions. When trace gas columns are considered, the relative importance of AOD decreases, and meteorological fields (e.g., V10M and planetary boundary layer) take precedence, implying that AOD and trace gas columns may contain redundant information. Meteorological fields and AODs are the most important factors for $PM_{2.5}$ estimates in Region W and Region N when trace gas columns are not available. But the trace gas columns (SO_2, NH_3, NO_2) are as important as the meteorological fields (V10M, U10M, PBLH) when they are taken into account, implying possible chemical reactions (e.g., formation of ammonium sulfate and nitrate) and physical processes (e.g., transport and dispersion) within the regions. The model trained from Region C (four regions as a whole) shows that AODs can explain a large fraction of the variance of $PM_{2.5}$ when trace gas columns are missing. However, with the presence of trace gas columns, meteorological fields are the most important factors that modulate $PM_{2.5}$ estimates. Similarly, this discrepancy could be attributed to the redundant information in AODs and trace gas columns. In a larger area (Region A), regardless of the presence of trace gas columns, meteorological fields are the dominant features. This result may be explained by the high correlation between AODs and all trace gas columns (Figure A1), which leads to features to be selected from either type as they contain similar information thus resulting in a lower overall ranking score for either feature type. Notably, while daily estimates indicate that emissions are the least important features in all cases, this could be because much of the predictive information can be inferred from the other features, due to a scarcity of varying emission data, or because the source at daily time scales does not change spatially as much in the model.

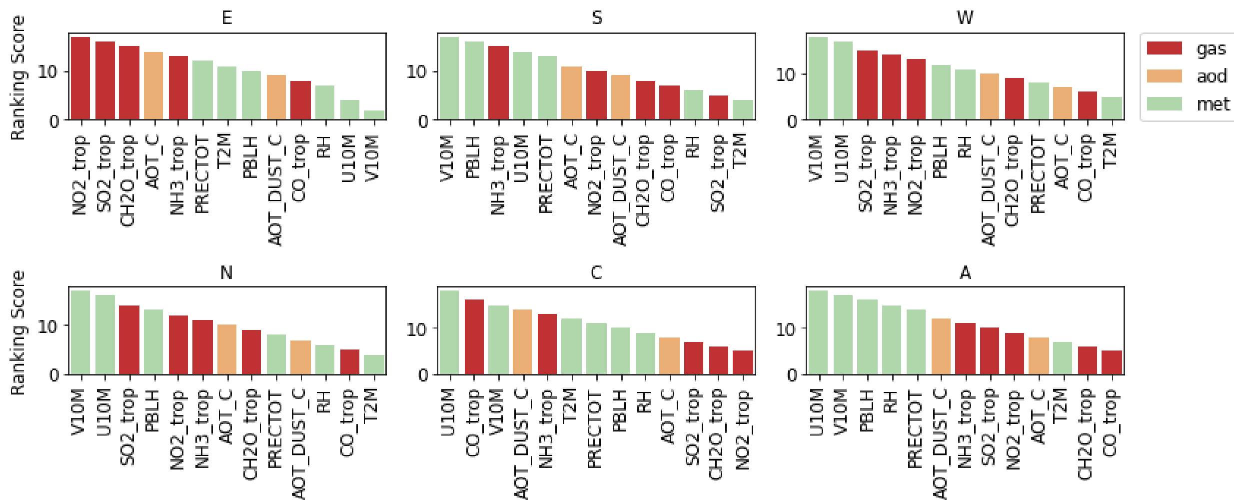

Figure 4. Ranking scores of features from AODs, meteorological fields, and trace gas columns in estimating daily $PM_{2.5}$. The ranking scores are derived from AutoML-trained "best estimators" that incorporate both trace gas columns and AOD, as well as meteorological fields and an emission inventory.

For monthly $PM_{2.5}$ estimates, although the patterns of the relative importance of different feature types remain similar among the four regions and Region C, the specific ranking order of features varies in different regions. The results can be partially related to the dominant sources. For example, a slightly lower mass fraction of sulfate in Region W (~13% in $PM_{2.5}$) compared to other regions (14%-17%) corresponds to a lower ranking score of “SO2_trop”. When building a model for a larger geospatial extent (Region A), the ranking score of meteorological fields declines. A possible reason is that the ML model for Region A assumes the same interactions among features for all regions and gives lower importance to meteorological variables compared to other types. But in reality, meteorology varies across the country and different meteorological factors may play different roles in different regions. On the other hand, monthly averaged precipitation and relative humidity in Region A are less correlated with $PM_{2.5}$ (Figure A2) than in other regions on monthly or daily scales, implying that information about processes (e.g., wet deposition) is diluted.

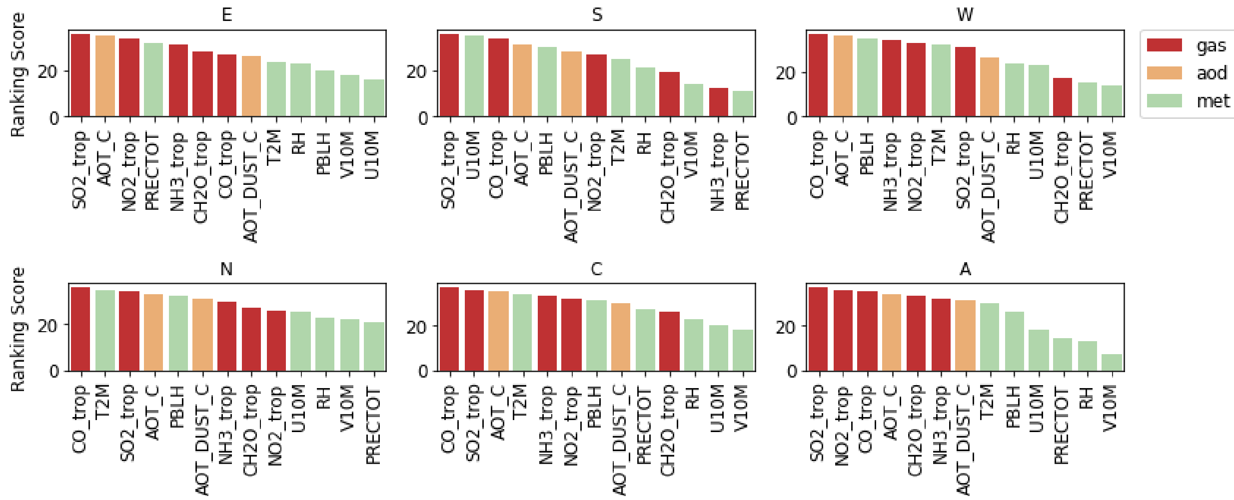

Figure 5. Ranking scores of features from AODs, meteorological fields, and trace gas columns in estimating monthly $PM_{2.5}$. The ranking scores are derived from AutoML-trained "best estimators" that incorporate both trace gas columns and AOD, as well as meteorological fields and an emission inventory.

3.3 Implications for $PM_{2.5}$ speciation

Along with the feature importance generated by AutoML, we use Spearman's rank correlation coefficient to infer the chemical composition of $PM_{2.5}$. Note that feature importance (or ranking score) and Spearman's rank correlation coefficient address different aspects. Feature importance concerns the interactions among features and features' contribution to the predictive capability, but it does not reveal the individual relationship between target variable and each feature. On the other hand, Spearman's rank measures the monotonic relationship (whether linear or not) between two variables but does not necessarily inform on its significance in a predictive model with other features. Here we show that, in the regions where trace gas columns are associated with higher ranking scores, the correlation between trace gas columns and $PM_{2.5}$ are also high. We find that tropospheric columns of SO_2 and NO_2 contribute most to the daily and monthly $PM_{2.5}$ estimates in Region E based on ranking scores, along with the highest Spearman's rank correlation coefficients. The agreement between AutoML and Spearman's rank correlation suggests secondary inorganic PM (sulfate and nitrate) are critical species modulating the $PM_{2.5}$ concentrations in Region E. Thus, the agreement between the ranking scores and the Spearman correlations provide evidence for chemical speciation of $PM_{2.5}$ and thus potential to infer source attribution in the subregions. Figure 6 also suggests that SO_2 (Region S) and CO (Region W and Region N) have higher correlation coefficients with $PM_{2.5}$ compared to other trace gas columns, consistent with the monthly ranking scores (Figure 5). The findings suggest that sulfate may modulate monthly $PM_{2.5}$ variability in Region S, whereas primary pollutant CO may modulate monthly $PM_{2.5}$ variability in Regions W and N.

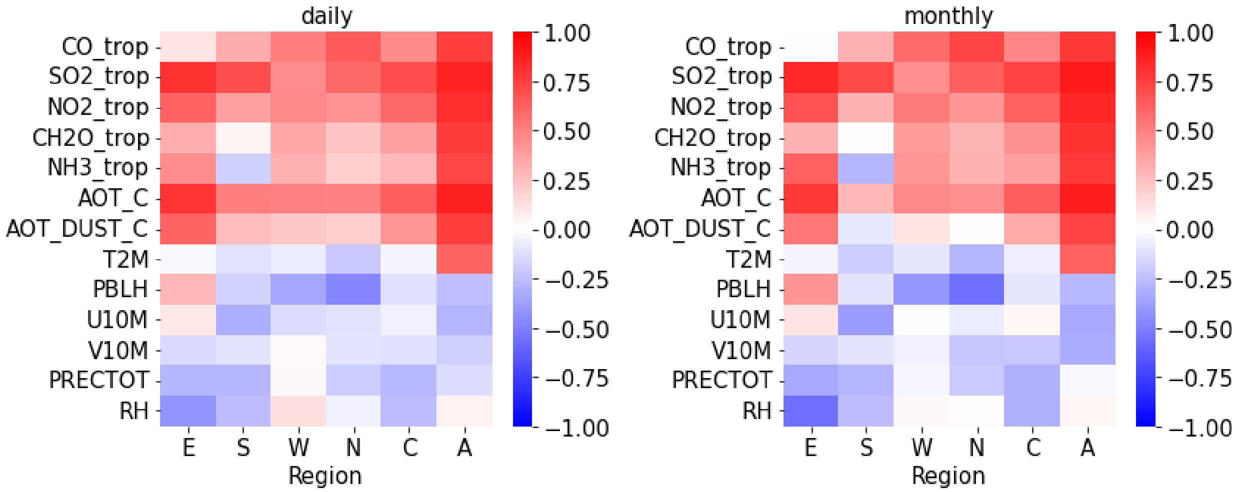

Figure 6. Spearman's rank correlation coefficient between $PM_{2.5}$ and AODs, meteorological fields, and trace gas columns.

3.4 AutoML consistently outperforms baseline machine learning models

We use the independent testing data to evaluate the advantage of using AutoML by comparing the "best estimator" from AutoML with LR and two commonly used nonlinear ML models: Random Forest (RF) and XGBoost (XGB). As expected, the performance of ML models varies case by case (Fig. 7a). For example, although the performance of RF is generally worse than XGBoost, it outperforms XGBoost when estimating monthly $PM_{2.5}$ in Region N. Therefore, it is not the best practice to implement the same machine learning algorithm for every region. Instead, the best estimators trained by AutoML outperform RF, XGBoost, and LR, especially at the regional scale. Because AutoML consists of a set of different learning algorithms and explores several possible hyperparameter combinations of each algorithm when training the estimators, it is at least no worse than a prior model selection and hyperparameter tuning (e.g., grid-search, random search, and bayesian search, etc.). We also show that an increase in data volume (e.g., daily compared to monthly) is likely to narrow the gap in R^2, highlighting the importance of attaining a large quantity of high-quality data for data-driven model development.

To assess whether trace gas columns can improve the $PM_{2.5}$ estimates, we repeat the regressions by implementing the above learning algorithms on a daily and monthly scale without trace gas columns, and calculate the difference in R^2 (Fig. 7b). We show that no matter the choice of learning algorithms, including trace gas columns consistently results in a higher R^2. Although the most obvious improvements come from LR, the best estimators from LR are in general worse than the nonlinear models, confirming that the assumption of a nonlinear relationship between features and $PM_{2.5}$ is more appropriate. In accordance with the present results, previous studies (e.g., Porter & Heald, 2019; Tai et al., 2010) have demonstrated that the correlations between PM and meteorological conditions are complex.

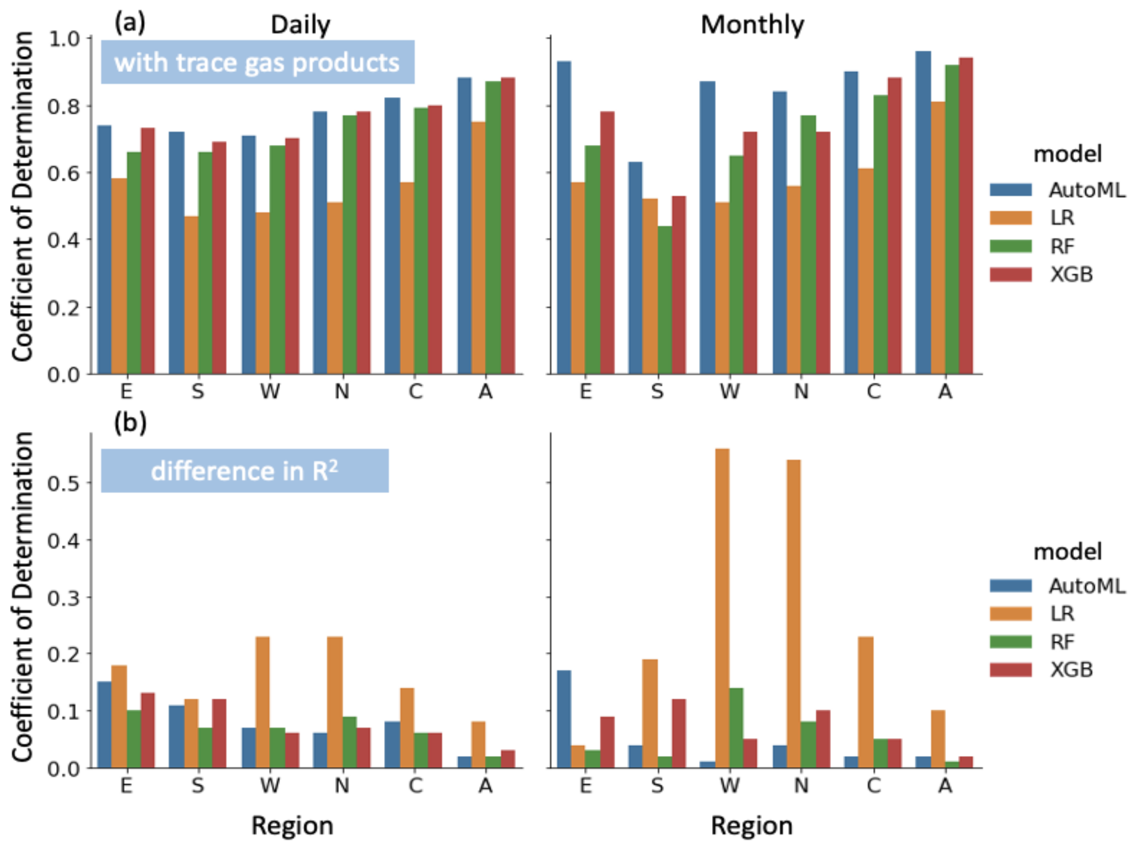

Figure 7. Performance of different estimators in estimating daily and monthly $PM_{2.5}$. (a) Estimators trained from the data with trace gas products; (b) Increases in R^2 from (a) compared to the estimators without considering trace gas products as features. Estimators are trained from Automated Machine Learning (AutoML), linear regression (LR), Random Forest (RF), and eXtreme Gradient Boosting (XGB).

3.5 Is "Big Data" always better?

The above analysis has shown that a larger volume of data at the same time scale (e.g., Region A) results in a better predictive capability compared to separate models for each of its subregions. However, such comparisons are potentially misleading, because the testing datasets are different and the averaging effect between regions of the metric. Two questions are raised here: (1) How well does a "generalized model" trained on the larger region perform when applied to the sub-regions it encompasses ("spatial mismatch")? (2) What role do trace gas products play in the application of a "spatially mismatched" model? Both questions are in line with the emphasis of Data-Centric AI, as a generalized model attempts to make use of the additional available samples to more robustly infer the predictive relationships, but it is possible that only a part of the data is indeed useful. On the other hand, while the first principle (e.g., chemical reactions) should be universal, due to incomplete features such as human activities, the underlying physical and chemical processes embedded in different places are distinct. For example, the models are unaware of prior knowledge such as the number of vehicles and power plants, and the complex regional meteorological processes, which would suggest using a model tailored to each region.

Here we assess the applicability of the “best estimators” trained from larger areas (Region A and Region C) by applying them back to the sub-regions (E, S, W, N). The results (Figure 8a) suggest that the generalized model (“a global model”) is not universally the best solution. For example, incorporating data from other regions (Region C) can improve the monthly $PM_{2.5}$ estimates in Region S, but the estimates suffer as a result of gaining more irrelevant data (Region A), implying that fundamentally different governing processes control $PM_{2.5}$ variability in that region. Such noise has the potential to mislead machine learning algorithms. On the contrary, the monthly $PM_{2.5}$ estimates in Region N benefit from more data. As a result, models that perform well at larger geographic scales may ensure generally good performance overall, but fail to capture the specificity in pollutant sources and meteorological processes for each of their subregions, because tailored models may be necessary if pollutant sources and meteorological processes vary from region to region. Even if we “mistakenly” apply the model across spatial scales, we find that the presence of trace gas columns benefits models (Figure 8b). In our cases, including trace gas columns as features does not impair predictive capability.

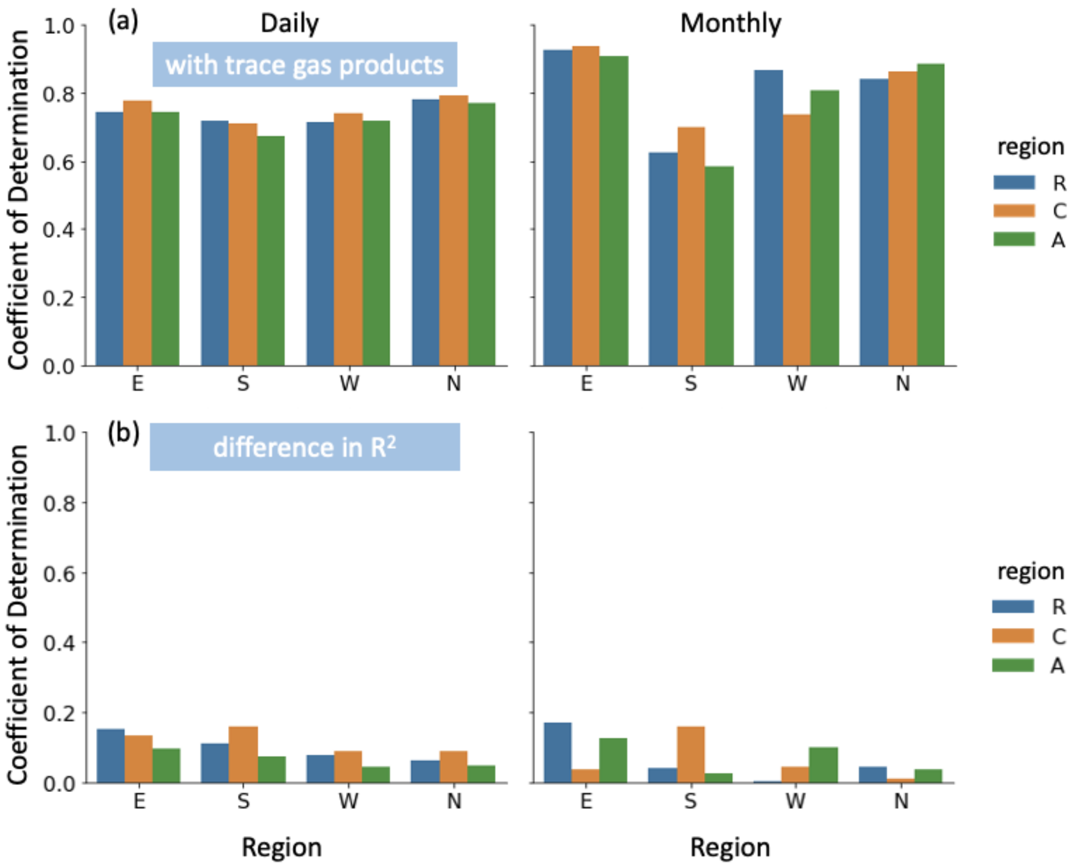

Figure 8. Performance of estimators in estimating daily and monthly $PM_{2.5}$ across spatial scales. (a) Estimators trained from the data with trace gas products; (b) Increases in R^2 from (a)

compared to the estimators without considering trace gas products as features. Estimators are trained from the region (R), the group of regions (C), and all land grid cells (A) and applied back to each region.

4 Conclusions

We use an Automated Machine Learning (AutoML) approach on a modeling testbed to evaluate the information content of tropospheric trace gas columns for fine particle estimates in India. We quantify the relative information content of trace gas columns, AODs, meteorological fields, and emissions for four sub-regions within India, and on daily versus monthly time scales. As a byproduct, an unsupervised-learning-based regionalization strategy is developed to delineate geographical regions with similar daily patterns of variability for analysis.

Our results suggest that incorporating trace gas modeled columns enhances $PM_{2.5}$ estimates in general, regardless of model assumptions. The enhancements in predictive capability differ in both space and time. Using the ranking scores and Spearman's rank correlation, we can infer the possible particle composition, and thus sources of $PM_{2.5}$. For example, we infer that $PM_{2.5}$ variability in Region E (see Figure 6) is modulated by secondary PM (sulfate and nitrate). However, in Region W and Region N, primary pollutants - as indicated by a strong correlation with CO - may modulate monthly $PM_{2.5}$ variability, whereas meteorological processes influence the daily $PM_{2.5}$ variability.

Our comparison of AutoML-derived models against selected baseline ML models demonstrates that AutoML is at least as good as a prior model selection and hyperparameter tuning. We ask the question "Is Big Data always better?" and find a nuanced answer that is regionally dependent. Even in these "spatially mismatched" models, however, we show that incorporating trace gas products can still improve $PM_{2.5}$ estimates across India.

The modeling testbed, like any other modeling-based study, is necessarily hampered by simulation accuracy. However, the idealized pseudo-observations used in this work provide a foundation for a better understanding of the importance of satellite retrievals of tropospheric trace gases for fine particle estimates in India, as well as the promising application of AutoML in atmospheric and environmental research. Future $PM_{2.5}$ estimates, for example, may benefit from the trace gas columns acquired by high-resolution geostationary satellites.

Data Availability

Scripts and data to reproduce the results and figures are preserved at https://doi.org/10.5281/zenodo.6363824 (Zheng, 2022) or https://github.com/zzheng93/code_DSI_India_AutoML. The raw data from GEOS-Chem simulations used for Automated Machine Learning and analysis in this study are available at https://doi.org/10.7916/nwx1-jt94 (Zheng et al., 2022).

Acknowledgments

We acknowledge ExxonMobil Research and Engineering Company and Data Science Institute (DSI) at Columbia University for supporting this work. We are grateful for helpful discussions with Drs. Ruth S. DeFries and Marianthi-Anna Kioumourtzoglou.

Appendix

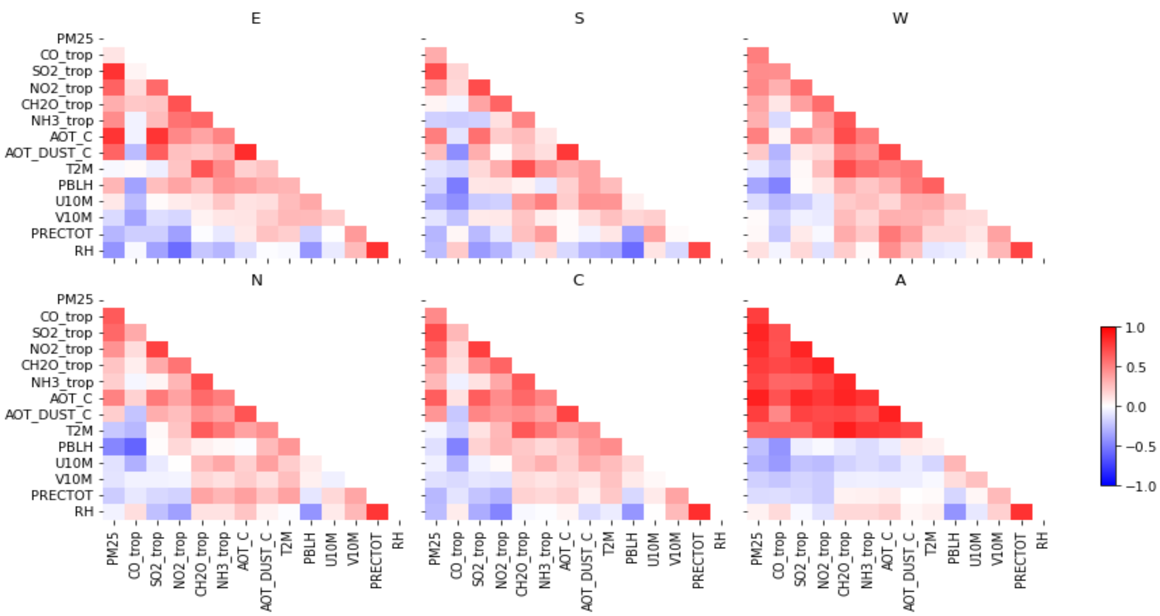

Figure A1. Spearman's rank correlation coefficient among $PM_{2.5}$, AODs, meteorological fields, and trace gas columns at the daily scale.

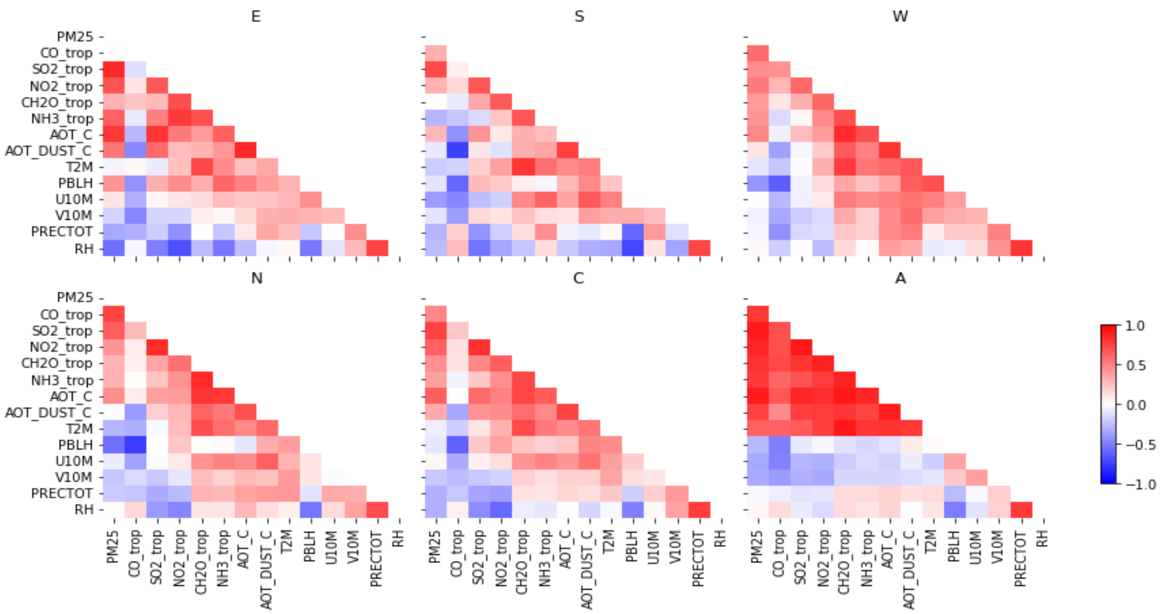

Figure A2. Spearman's rank correlation coefficient among $PM_{2.5}$, AODs, meteorological fields, and trace gas columns at the monthly scale.

References

Adams, M. D., Massey, F., Chastko, K., & Cupini, C. (2020). Spatial modelling of particulate matter air pollution sensor measurements collected by community scientists while cycling, land use regression with spatial cross-validation, and applications of machine learning for data correction. *Atmospheric Environment*, *230*, 117479. https://doi.org/10.1016/j.atmosenv.2020.117479

Agrawal, S., Barrington, L., Bromberg, C., Burge, J., Gazen, C., & Hickey, J. (2019). Machine Learning for Precipitation Nowcasting from Radar Images. *ArXiv:1912.12132 [Cs, Stat]*. Retrieved from http://arxiv.org/abs/1912.12132

Bali, K., Dey, S., & Ganguly, D. (2021). Diurnal patterns in ambient PM2.5 exposure over India using MERRA-2 reanalysis data. *Atmospheric Environment*, *248*, 118180. https://doi.org/10.1016/j.atmosenv.2020.118180

Brauer, M., Freedman, G., Frostad, J., van Donkelaar, A., Martin, R. V., Dentener, F., et al. (2016). Ambient Air Pollution Exposure Estimation for the Global Burden of Disease 2013. *Environmental Science & Technology*, *50*(1), 79–88. https://doi.org/10.1021/acs.est.5b03709

Brauer, M., Guttikunda, S. K., K A, N., Dey, S., Tripathi, S. N., Weagle, C., & Martin, R. V. (2019). Examination of monitoring approaches for ambient air pollution: A case study for India. *Atmospheric Environment*, *216*, 116940. https://doi.org/10.1016/j.atmosenv.2019.116940

Breiman, L. (2001). Random Forests. *Machine Learning*, *45*(1), 5–32. https://doi.org/10.1023/A:1010933404324

Chaliyakunnel, S., Millet, D. B., & Chen, X. (2019). Constraining Emissions of Volatile Organic Compounds Over the Indian Subcontinent Using Space-Based Formaldehyde Measurements. *Journal of Geophysical Research: Atmospheres*, *124*(19), 10525–10545. https://doi.org/10.1029/2019JD031262

Chen, T., & Guestrin, C. (2016). XGBoost: A Scalable Tree Boosting System. In *Proceedings of the 22nd ACM SIGKDD International Conference on Knowledge Discovery and Data Mining* (pp. 785–794). San Francisco, California, USA: ACM Press. https://doi.org/10.1145/2939672.2939785

Chowdhury, S., Dey, S., Guttikunda, S., Pillarisetti, A., Smith, K. R., & Di Girolamo, L. (2019). Indian annual ambient air quality standard is achievable by completely mitigating emissions from household sources. *Proceedings of the National Academy of Sciences*, *116*(22), 10711–10716. https://doi.org/10.1073/pnas.1900888116

Curci, G., Hogrefe, C., Bianconi, R., Im, U., Balzarini, A., Baró, R., et al. (2015). Uncertainties of simulated aerosol optical properties induced by assumptions on aerosol physical and chemical properties: An AQMEII-2 perspective. *Atmospheric Environment*, *115*, 541–552. https://doi.org/10.1016/j.atmosenv.2014.09.009

Di, Q., Amini, H., Shi, L., Kloog, I., Silvern, R., Kelly, J., et al. (2019). An ensemble-based model of PM2.5 concentration across the contiguous United States with high spatiotemporal resolution. *Environment International*, *130*, 104909. https://doi.org/10.1016/j.envint.2019.104909

van Donkelaar, A., Martin, R. V., & Park, R. J. (2006). Estimating ground-level PM $_{2.5}$ using aerosol optical depth determined from satellite remote sensing. *Journal of Geophysical Research*, *111*(D21), D21201. https://doi.org/10.1029/2005JD006996

Fiore, A. M., Jacob, D. J., Mathur, R., & Martin, R. V. (2003). Application of empirical orthogonal functions to evaluate ozone simulations with regional and global models. *Journal of Geophysical Research: Atmospheres*, *108*(D14), 4431. https://doi.org/10.1029/2002JD003151

Fiore, A. M., Milly, G. P., Quiñones, L., Bowden, J., Hancock, S. E., Helstrom, E., et al. (2021). *Characterizing Changes in Eastern U.S. Pollution Events in a Warming World* (preprint). Atmospheric Sciences. https://doi.org/10.1002/essoar.10508944.1

Geng, G., Meng, X., He, K., & Liu, Y. (2020). Random forest models for PM2.5 speciation concentrations using {MISR} fractional AODs. *Environmental Research Letters*, *15*(3), 034056. https://doi.org/10.1088/1748-9326/ab76df

Gentine, P., Eyring, V., & Beucler, T. (2021). Deep Learning for the Parametrization of Subgrid Processes in Climate Models. In G. Camps-Valls, D. Tuia, X. X. Zhu, & M. Reichstein (Eds.), *Deep Learning for the Earth Sciences* (1st ed., pp. 307–314). Wiley. https://doi.org/10.1002/9781119646181.ch21

Geurts, P., Ernst, D., & Wehenkel, L. (2006). Extremely randomized trees. *Machine Learning*, *63*(1), 3–42. https://doi.org/10.1007/s10994-006-6226-1

Greenstone, M., Nilekani, J., Pande, R., Ryan, N., Sudarshan, A., & Sugathan, A. (2015). Lower pollution, longer lives: life expectancy gains if India reduced particulate matter pollution. *Economic and Political Weekly*, 40–46.

Hastie, T., Tibshirani, R., & Friedman, J. (2009). *The Elements of Statistical Learning*. New York, NY: Springer New York. https://doi.org/10.1007/978-0-387-84858-7

Hoff, R. M., & Christopher, S. A. (2009). Remote Sensing of Particulate Pollution from Space: Have We Reached the Promised Land? *Journal of the Air & Waste Management Association*, *59*(6), 645–675. https://doi.org/10.3155/1047-3289.59.6.645

Hu, X., Belle, J. H., Meng, X., Wildani, A., Waller, L. A., Strickland, M. J., & Liu, Y. (2017). Estimating PM2.5 Concentrations in the Conterminous United States Using the Random Forest Approach. *Environmental Science & Technology*, *51*(12), 6936–6944. https://doi.org/10.1021/acs.est.7b01210

Hutter, F., Kotthoff, L., & Vanschoren, J. (Eds.). (2019). *Automated Machine Learning: Methods, Systems, Challenges*. Cham: Springer International Publishing. https://doi.org/10.1007/978-3-030-05318-5

Irrgang, C., Boers, N., Sonnewald, M., Barnes, E. A., Kadow, C., Staneva, J., & Saynisch-Wagner, J. (2021). Towards neural Earth system modelling by integrating artificial intelligence in Earth system science. *Nature Machine Intelligence*, *3*(8), 667–674. https://doi.org/10.1038/s42256-021-00374-3

Karambelas, A., Holloway, T., Kinney, P. L., Fiore, A. M., DeFries, R., Kiesewetter, G., & Heyes, C. (2018). Urban versus rural health impacts attributable to $PM_{2.5}$ and O_3 in northern India. *Environmental Research Letters*, *13*(6), 064010. https://doi.org/10.1088/1748-9326/aac24d

Karambelas, A., Fiore, A. M., Westervelt, D. M., McNeill, V. F., Randles, C. A., Venkataraman, C., et al. (2022). Investigating drivers of particulate matter pollution over India and the implications for radiative forcing with GEOS-Chem-TOMAS15. *Submitted*.

Ke, G., Meng, Q., Finley, T., Wang, T., Chen, W., Ma, W., et al. (2017). LightGBM: A highly efficient gradient boosting decision tree. In I. Guyon, U. V. Luxburg, S. Bengio, H. Wallach, R. Fergus, S. Vishwanathan, & R. Garnett (Eds.), *Advances in neural information processing systems* (Vol. 30). Curran Associates, Inc. Retrieved from https://proceedings.neurips.cc/paper/2017/file/6449f44a102fde848669bdd9eb6b76fa-Paper.pdf

Keller, C. A., Long, M. S., Yantosca, R. M., Da Silva, A. M., Pawson, S., & Jacob, D. J. (2014). HEMCO v1.0: a versatile, ESMF-compliant component for calculating emissions in atmospheric models. *Geoscientific Model Development*, *7*(4), 1409–1417. https://doi.org/10.5194/gmd-7-1409-2014

Kumar, J., Mills, R. T., Hoffman, F. M., & Hargrove, W. W. (2011). Parallel k-Means Clustering for Quantitative Ecoregion Delineation Using Large Data Sets. *Procedia Computer Science*, *4*, 1602–1611. https://doi.org/10.1016/j.procs.2011.04.173

Labe, Z. M., & Barnes, E. A. (2021). Detecting Climate Signals Using Explainable AI With Single-Forcing Large Ensembles. *Journal of Advances in Modeling Earth Systems*, *13*(6). https://doi.org/10.1029/2021MS002464

Lagerquist, R., McGovern, A., & Gagne II, D. J. (2019). Deep Learning for Spatially Explicit Prediction of Synoptic-Scale Fronts. *Weather and Forecasting*, *34*(4), 1137–1160. https://doi.org/10.1175/WAF-D-18-0183.1

Lian, T., & Chen, D. (2012). An Evaluation of Rotated EOF Analysis and Its Application to Tropical Pacific SST Variability. *Journal of Climate*, *25*(15), 5361–5373. https://doi.org/10.1175/JCLI-D-11-00663.1

McGovern, A., Elmore, K. L., Gagne, D. J., Haupt, S. E., Karstens, C. D., Lagerquist, R., et al. (2017). Using Artificial Intelligence to Improve Real-Time Decision-Making for High-Impact Weather. *Bulletin of the American Meteorological Society*, *98*(10), 2073–2090. https://doi.org/10.1175/BAMS-D-16-0123.1

Pai, S. J., Heald, C. L., Pierce, J. R., Farina, S. C., Marais, E. A., Jimenez, J. L., et al. (2020). An evaluation of global organic aerosol schemes using airborne observations. *Atmospheric Chemistry and Physics*, *20*(5), 2637–2665. https://doi.org/10.5194/acp-20-2637-2020

Porter, W. C., & Heald, C. L. (2019). The mechanisms and meteorological drivers of the summertime ozone–temperature relationship. *Atmospheric Chemistry and Physics*, *19*(21), 13367–13381. https://doi.org/10.5194/acp-19-13367-2019

Prashanth, P., Speth, R. L., Eastham, S. D., Sabnis, J. S., & Barrett, S. R. H. (2021). Post-combustion emissions control in aero-gas turbine engines. *Energy & Environmental Science*, *14*(2), 916–930. https://doi.org/10.1039/D0EE02362K

Prokhorenkova, L., Gusev, G., Vorobev, A., Dorogush, A. V., & Gulin, A. (2018). CatBoost: unbiased boosting with categorical features. In S. Bengio, H. Wallach, H. Larochelle, K. Grauman, N. Cesa-Bianchi, & R. Garnett (Eds.), *Advances in neural information processing systems* (Vol. 31). Curran Associates, Inc. Retrieved from https://proceedings.neurips.cc/paper/2018/file/14491b756b3a51daac41c24863285549-Paper.pdf

Ravishankara, A. R., David, L. M., Pierce, J. R., & Venkataraman, C. (2020). Outdoor air pollution in India is not only an urban problem. *Proceedings of the National Academy of Sciences*, *117*(46), 28640–28644. https://doi.org/10.1073/pnas.2007236117

Reichstein, M., Camps-Valls, G., Stevens, B., Jung, M., Denzler, J., Carvalhais, N., & Prabhat. (2019). Deep learning and process understanding for data-driven Earth system science. *Nature*, *566*(7743), 195–204. https://doi.org/10.1038/s41586-019-0912-1

Rybarczyk, Y., & Zalakeviciute, R. (2018). Machine Learning Approaches for Outdoor Air Quality Modelling: A Systematic Review. *Applied Sciences*, *8*(12), 2570. https://doi.org/10.3390/app8122570

Shi, W., & Zeng, W. (2014). Application of k-means clustering to environmental risk zoning of the chemical industrial area. *Frontiers of Environmental Science & Engineering*, *8*(1), 117–127. https://doi.org/10.1007/s11783-013-0581-5

Stohl, A., Aamaas, B., Amann, M., Baker, L. H., Bellouin, N., Berntsen, T. K., et al. (2015). Evaluating the climate and air quality impacts of short-lived pollutants. *Atmospheric Chemistry and Physics*, *15*(18), 10529–10566. https://doi.org/10.5194/acp-15-10529-2015

Tai, A. P. K., Mickley, L. J., & Jacob, D. J. (2010). Correlations between fine particulate matter (PM2.5) and meteorological variables in the United States: Implications for the sensitivity of PM2.5 to climate change. *Atmospheric Environment*, *44*(32), 3976–3984. https://doi.org/10.1016/j.atmosenv.2010.06.060

The International GEOS-Chem User. (2018). *Geoschem/Geos-Chem: Geos-Chem 12.0.2 Release*. Zenodo. https://doi.org/10.5281/ZENODO.1455215

Toms, B. A., Barnes, E. A., & Ebert-Uphoff, I. (2020). Physically Interpretable Neural Networks for the Geosciences: Applications to Earth System Variability. *Journal of Advances in Modeling Earth Systems*, *12*(9). https://doi.org/10.1029/2019MS002002

Wang, C., Wu, Q., Weimer, M., & Zhu, E. (2021). FLAML: A fast and lightweight AutoML library. In *MLSys*.

Wolpert, D. H. (1996). The Lack of A Priori Distinctions Between Learning Algorithms. *Neural Computation*, *8*(7), 1341–1390. https://doi.org/10.1162/neco.1996.8.7.1341

World Health Organization. (2021). WHO global air quality guidelines: particulate matter (PM2.5 and PM10), ozone, nitrogen dioxide, sulfur dioxide and carbon monoxide: executive summary. World Health Organization.

Xiao, Q., Chang, H. H., Geng, G., & Liu, Y. (2018). An Ensemble Machine-Learning Model To Predict Historical PM2.5 Concentrations in China from Satellite Data. *Environmental Science & Technology*, *52*(22), 13260–13269. https://doi.org/10.1021/acs.est.8b02917

Xu, J.-W., Martin, R. V., van Donkelaar, A., Kim, J., Choi, M., Zhang, Q., et al. (2015). Estimating ground-level PM_{2.5} in eastern China using aerosol optical depth determined from the GOCI satellite instrument. *Atmospheric Chemistry and Physics*, *15*(22), 13133–13144. https://doi.org/10.5194/acp-15-13133-2015

Zheng, Z. (2022). zzheng93/code_DSI_India_AutoML: First release (Version v0.0.0). Zenodo. https://doi.org/10.5281/ZENODO.6363824

Zheng, Z., Ching, J., Curtis, J. H., Yao, Y., Xu, P., West, M., & Riemer, N. (2020). Unsupervised Regionalization of Particle-resolved Aerosol Mixing State Indices on the Global Scale. *ArXiv:2012.03365 [Physics]*. Retrieved from http://arxiv.org/abs/2012.03365

Zheng, Z., Fiore, A. M., Westervelt, D. M., Milly, G. P., Goldsmith, Karambelas, A., et al. (2022). Automated machine learning to evaluate the information content of tropospheric trace gas columns for fine particle estimates over India: a modeling testbed [Data set]. Columbia University. https://doi.org/10.7916/NWX1-JT94